

Physical interpretation of the $2s$ excitation of the nucleon

Finn M. Stokes, Waseem Kamleh, Derek B. Leinweber,
Benjamin J. Owen[‡]

ARC Special Research Centre for the Subatomic Structure of Matter (CSSM), Department of Physics, The University of Adelaide, SA, 5005, Australia.

E-mail: finn.stokes@adelaide.edu.au

Abstract. Lattice QCD calculations of the $2s$ radial excitation of the nucleon place the state at an energy of approximately 1.9 GeV, raising the possibility that it is associated with the $N1/2^+(1880)$ and $N1/2^+(1710)$ resonances through mixing with two-particle meson-baryon states. The discovery of the $N1/2^+(1880)$ resonance in pion photoproduction but not in πN scattering and the small width of the $N1/2^+(1710)$ resonance suggest that a state associated with these resonances would be insensitive to the manner in which pions are permitted to dress it. To explore this possibility, we examine the spectrum of nucleon radial excitations in both 2+1 flavour QCD and in simulations where the coupling to meson-baryon states is significantly modified through quenching. We find the energy of the $2s$ radial excitation to be insensitive to this modification for quark masses close to the physical point. This invariance provides further evidence that the $2s$ radial excitation of the nucleon is associated with the $N1/2^+(1880)$ and $N1/2^+(1710)$ resonances.

Keywords: lattice QCD, hadron spectroscopy, variational method, radial excitations

1. Introduction

1.1. First radial excitation of the nucleon in lattice QCD

The realisation that the Roper resonance is not the anticipated $2s$ radial excitation of a constituent quark model was established almost a decade ago [1] as it became apparent that the Roper is dynamically generated through rescattering in the πN , $\pi\Delta$, and σN channels [2]. This conclusion is driven by lattice QCD calculations showing the $2s$ radial excitation of the nucleon lies at approximately 1.9 GeV [1–14], far from the Roper resonance of the nucleon at 1.44 GeV [15].

The first hint of a surprise in the $2s$ excitation energy was reported in Ref. [3]. By combining narrow and wide Gaussian-smearred sources with opposite signs, a node in the wave function of the quark distributions could be created. The generalised eigenvalue solution [16, 17] determined the superposition of Gaussian-smearred quark sources and the $2s$ radial excitation of the nucleon was observed at 1.79(8) GeV in a lattice volume of 3 fm on a side [4].

These first results were confirmed by the HSC collaboration at heavy quark masses [18] and in an approach using the Athens Model Independent Analysis Scheme [5] to extract the spectrum from lattice correlation functions. A comprehensive analysis of the structure and flow of the states as a function of quark mass followed in Ref. [6]. The wave functions of both the $2s$ and $3s$ excitations were calculated in lattice QCD [7, 8] and their profiles were found to compare well with constituent quark model expectations [7].

Next generation calculations appeared in 2016 with a high-statistics calculation coming from the CSSM [2] placing the $2s$ state at 1.90(6) GeV on the 3 fm lattice. More exotic five-quark descriptions for the Roper resonance were pursued [9, 10]. However, no new low-lying states have been observed. Similarly, the consideration of hybrid baryons [11] has not revealed any new low-lying states in the Roper region.

[‡] Now at the Bureau of Meteorology, Adelaide, SA, Australia.

This situation contrasts the case of the $\Lambda(1405)$ channel. There, three-quark operators are able to excite a finite-volume state in the resonance region of ~ 1.4 GeV. Lattice QCD calculations of the electromagnetic form factors of this state show a localised state similar in size to the ground-state Λ baryon [19]. However, it is the quark mass dependence of the magnetic form factor that signals the presence of a molecular meson-baryon bound state in the finite-volume of the lattice [20, 21].

1.2. Other evidence supporting the $2s$ excitation at ~ 2 GeV

The very first insights into the role of two-particle scattering states in the Roper resonance region appeared from Lang *et al.* [12]. Scattering states very near the non-interacting two particle energies were observed. While not manifesting any obvious resonance signature, an HEFT analysis bringing experimental phase shifts and inelasticities to the finite volume of the lattice [22] illustrates how Lang *et al.*'s results are in accord with the scattering phase-shifts and inelasticities in the Roper resonance region. The most recent calculations of the nucleon spectrum are focused on precision calculations of the very lowest-lying scattering states [23–25].

In addition, the three-quark single particle state was observed in Lang *et al.*'s analysis. Its position persists at the order of 2 GeV, even when lower-lying scattering states are included in the correlation matrix, thus confirming earlier observations [1, 4–10],

The role of chiral symmetry in lattice fermion actions has also been explored quantitatively in Ref. [26] to see if the explicit breaking of chiral symmetry in Wilson-clover fermion actions is responsible for the large $2s$ excitation energy. A direct analysis of lattice correlation functions from Wilson-clover and overlap fermion actions – the latter providing a lattice implementation of chiral symmetry – reveals no differences in the spectrum.

Since then, parity-expanded variational analysis (PEVA) techniques [27] have been developed to explore the electromagnetic form factors of both the even and odd-parity excitations of the nucleon [13] and their electromagnetic transitions to the ground state [28]. With regard to the $2s$ excitation, the charge radius of the excited proton is larger than the ground state, in accord with expectations. Moreover, the magnetic moments of the excited $2s$ proton and neutron calculated in lattice QCD agree with the ground-state magnetic moments, again consistent with the expectations of a $2s$ excitation.

In summary, the $2s$ radial excitation of the nucleon observed in lattice QCD is firmly entrenched at approximately 2 GeV. The most precise determination [2] places it at 1.90(6) GeV in a 3 fm lattice volume. The single-particle basis state contribution in the Roper resonance energy regime is a few percent at best [22]. In the literature, the $2s$ quark-model excitation is often referred to as the Roper state. We now know this is not the case. But then, what state(s) in the nucleon spectrum are associated with the $2s$ single-particle excitation of the nucleon?

1.3. $N1/2^+(1710)$ and $N1/2^+(1880)$ resonances

With the $2s$ radial excitation at ~ 2 GeV near the physical point, we turn our attention to nucleon resonances in this energy regime. As the single-particle quark model state mixes with nearby two-particle states to form resonances, we anticipate the $2s$ radial excitation is largely associated with the $N1/2^+(1880)$ resonance observed in meson photoproduction [29] and to some extent the $N1/2^+(1710)$ as it is only 170 MeV away.

The $N1/2^+(1710)$ resonance has a small width of 80 to 200 MeV [30] relative to the Roper resonance for example at 250 to 450 MeV. Moreover, the πN partial width of the $N1/2^+(1710)$ is in the range of 5 to 20%. Within the finite volume of the lattice, these resonance properties suggest that the $2s$ excitation may have relatively weak coupling to the long-range πN components. The $N1/2^+(1880)$ resonance is a curious state that was not seen in πN scattering experiments. Rather it was discovered through $\gamma p \rightarrow K^+ \Lambda$ photoproduction experiments [29]. While its width is estimated at 200 to 400 MeV, the πN partial width may be as small as 3% [30], in accord with its lack of signature in πN scattering. Again, these resonance properties suggest that the $2s$ excitation observed on the lattice may have relatively weak coupling to the long-range πN components.

This admits the possibility of an insensitivity of the $2s$ radial excitation energy to changes to the manner in which meson-baryon states dress the state observed on the lattice. One could probe this possibility by altering these dressings and measuring the impact of these alterations on the observed spectrum.

In short, if the finite-volume $2s$ state observed in lattice QCD is associated with the $N1/2^+(1710)$ and $N1/2^+(1880)$ resonances, there is good reason to anticipate that the mass of the state is insensitive to modifications of the meson cloud dressing. This possibility is explored herein.

1.4. Modifying the meson-baryon couplings

Our approach is to significantly modify the strength of meson-baryon two-particle couplings to the eigenstates of the finite-volume nucleon spectrum and search for the existence of states insensitive to this variation. We implement this by removing sea-quark-loops from the gauge field generation, eliminating a class of quark-flow diagrams and thus suppressing the meson-baryon couplings.

The phenomenology of this quenching is well understood through the formalism of (partially) quenched chiral perturbation theory for baryons [31,32]. A comprehensive analysis of baryon couplings and their modifications under quenching is provided in Ref. [33]. The changes are complicated, with some meson dressings changing in sign and most dressings becoming significantly suppressed.

For example, consider the pion dressings of the proton. Table 1 of Ref. [34] provides the contributions of connected and disconnected quark flows. The disconnected contributions disappear upon quenching the theory, but the connected contributions remain. The sum of all of these contributions is 5.38, whereas the connected contributions alone sum to 1.50§. Consequentially, quenching reduces the coupling by a factor of 3.6.

It is well known that ground state hadrons such as the nucleon are approximated well by quenched QCD [35,36], with a precision of ~ 1 to 3% [37]. The success for the lowest-lying hadrons is associated with the dominance of a single-particle basis state in their structure. This single-particle dominance is evident in Hamiltonian Effective Field Theory (HEFT). As illustrated in Fig. 10a of Ref. [2], HEFT describes the ground-state nucleon as 78% single-particle basis state.

The $2s$ excitation displays a somewhat similar superposition of basis states in HEFT. For example, Fig. 5 of Ref. [22] illustrates that the single-particle basis state component of the $2s$ excitation may approach 70%, with 25% in the $\pi\Delta$ channel, and only a few percent in the long-range πN and σN channels.

With 70% of the state composition insensitive to the meson-baryon basis-state components, one can see how quenching the theory would generate relatively small changes, particularly if the lattice scale determination is designed to preserve the physics of full QCD at a physically relevant scale.

To this end, we use the Sommer scale [38] which sets the lattice spacing by preserving the force of the static quark potential at a scale relative to ground-state hadronic physics. In this way, the physics at that scale is preserved. However, changes in the pion-nucleon couplings to states, for example, mean that the long-distance part of the state is different.

2. Correlation Matrix Techniques

To isolate energy eigenstates on the lattice, we use the variational method [16,17], briefly reviewed in the following. To access N states of the spectrum, one requires a minimum of N interpolators coupling well to the states of interest. The parity-projected two-point correlation matrix for $\vec{p} = 0$ is introduced as

$$G_{ij}^{\pm}(t) = \sum_{\vec{x}} \text{Tr}_{\text{sp}} \{ \Gamma_{\pm} \langle \Omega | \chi_i(x) \bar{\chi}_j(0) | \Omega \rangle \}, \quad (1)$$

$$\approx \sum_{\alpha=0}^{N-1} \lambda_i^{\alpha} \bar{\lambda}_j^{\alpha} e^{-m_{\alpha} t}, \quad (2)$$

§ In a scheme where the physical $n\pi^+$ dressing of the proton is equal to $2(D+F)^2 = 2g_A^2$ with $g_A = 1.27$

where χ_i and $\bar{\chi}_j$ are proton interpolating fields at the sink and source respectively, $|\Omega\rangle$ denotes the non-trivial ground-state fields, $\Gamma_{\pm} = (\gamma_0 \pm 1)/2$ projects the parity of the eigenstates, λ_i^α and $\bar{\lambda}_j^\alpha$ are the couplings of the interpolators to the state with mass m_α , and α enumerates the energy eigenstates with the ground state corresponding to $\alpha = 0$. We use the Pauli representation of the γ matrices such that they are Hermitian. Dirac indices are implicit.

Using an average of $\{U\} + \{U^*\}$ configurations, our construction of $G_{ij}^\pm(t)$ is symmetric and real. We enforce this symmetry by working with an improved unbiased symmetric construction $(G_{ij} + G_{ji})/2$. To ensure that the matrix elements are $\sim \mathcal{O}(1)$, each element of $G_{ij}(t)$ is normalised by the diagonal elements of G_{ij} as $G_{ij}(t)/(\sqrt{G_{ii}(t_N)}\sqrt{G_{jj}(t_N)})$ (no sum on i or j) with normalisation time t_N at one time slice after the source.

An operator creating state α can be constructed as $\bar{\phi}^\alpha = \sum_j \bar{\chi}_j u_j^\alpha$, with linear coefficients u_j for each state α . As the time dependence of the two-point function is then governed by $\exp(-m_\alpha t)$ a recurrence relation can be used to solve for u_j^α

$$G_{ij}(t_0 + \Delta t) u_j^\alpha = e^{-m_\alpha \Delta t} G_{ij}(t_0) u_j^\alpha. \quad (3)$$

Multiplying from the left by $G^{-1}(t_0)$ provides the right eigenvector equation for u_j^α

$$[(G(t_0))^{-1} G(t_0 + \Delta t)]_{ij} u_j^\alpha = c^\alpha u_i^\alpha, \quad (4)$$

with $c^\alpha = e^{-m_\alpha \Delta t}$. Similarly, an operator annihilating state α can be defined as $\phi^\alpha = \sum_j \chi_j v_j^\alpha$, where v_j^α is given by the left eigenvalue equation

$$v_i^\alpha [G(t_0 + \Delta t) (G(t_0))^{-1}]_{ij} = c^\alpha v_j^\alpha. \quad (5)$$

The eigenvectors for state α , u_j^α and v_i^α , are then combined to create the eigenstate projected correlation function

$$G_\pm^\alpha(t) \equiv v_i^\alpha G_{ij}^\pm(t) u_j^\alpha, \quad (6)$$

with parity \pm . We note that with our symmetric construction for $G_{ij}^\pm(t)$, the left and right eigenvectors are equal.

In exciting the nucleon, we consider the standard local interpolating fields describing the quantum numbers of the proton

$$\chi_1(x) = \epsilon^{abc} (u^{a\tau}(x) C \gamma_5 d^b(x)) u^c(x), \text{ and} \quad (7)$$

$$\chi_2(x) = \epsilon^{abc} (u^{a\tau}(x) C d^b(x)) \gamma_5 u^c(x). \quad (8)$$

Here $u(x)$ and $d(x)$ represent the Dirac spinor for a single u or d quark at spacetime position x carrying a colour index a, b, c . The matrix C is the charge conjugation matrix and ϵ is the Levi-Cevita antisymmetric tensor. Gauge-invariant Gaussian smearing [39] is used to enlarge the basis of operators. Four different smearing levels are used at the fermion source and sink for each of the two nucleon interpolators, providing an 8×8 basis.

The effective mass function is defined as

$$M_{\text{eff}}(t) = \frac{1}{n} \log \left(\frac{G(t)}{G(t+n)} \right). \quad (9)$$

We consider $n = 2$ as it provides a more accurate estimation of the local slope of the projected correlator, while maintaining a good sample of points to identify plateau behaviour. A second-order single-elimination jackknife analysis [40] is used to calculate uncertainties with the χ^2/dof obtained via the full covariance matrix analysis.

Its well known that scattering states can contaminate the correlation functions of local single-particle operators. The standard nucleon interpolators used here favour localised states and tend to miss the non-local scattering states [4, 6, 9, 10, 41, 42], making the lattice spectrum incomplete. In this case there may be concern that the lattice energy levels extracted might be systematically contaminated from the missed levels.

The CSSM collaboration has explored this in detail [9, 10, 42] and has developed methods that ensure these systematic errors are suppressed through Euclidean time evolution. The use of a single-state Ansatz and a full covariance-matrix calculation of the χ^2/dof with a conservative cutoff of $\chi^2/\text{dof} < 1.2$ ensures that any remaining contamination is contained within the error bars reported [10].

Table 1. The relationship between hopping parameter values established in the PACS-CS [43] dynamical fermion ensembles, κ_D , and determined in quenched QCD, κ_Q , by matching the pion mass. The quenched ensembles are simulated with the Iwasaki action at $\beta = 2.58$ to provide a lattice spacing of $a = 0.100$ fm. The PACS-CS ensembles are labelled by the pion mass in the PACS-CS scheme. Lattice spacings for the dynamical ensembles, a_D , are provided in the Sommer scheme [38] with $r_0 = 0.4921(64)(+74)(-2)$ fm. The dynamical fermion ensembles contain n_D^{cfg} gauge field configurations with n_D^{src} sources computed on each configuration, and the quenched ensembles similarly for n_Q^{cfg} and n_Q^{src} .

m_π/MeV	a_D/fm	κ_D	n_D^{cfg}	n_D^{src}	κ_Q	n_Q^{cfg}	n_Q^{src}
701	0.102	0.13700	399	1	0.12409	350	1
570	0.101	0.13727	397	1	0.12453	350	1
411	0.096	0.13754	449	2	0.12495	350	1
296	0.095	0.13770	400	4	0.12522	350	1
156	0.093	0.13781	197	8	0.12539	350	1

3. Simulation Details

Our full QCD calculations are performed on the PACS-CS Collaboration’s gauge-field ensembles [43] made available via the ILDG [44]. These configurations make use of the Iwasaki gauge action [45] and an $\mathcal{O}(a)$ -improved Wilson quark action with Clover coefficient $C_{\text{SW}} = 1.715$. The masses of the up and down quarks are taken to be degenerate. The simulations use a fixed value of $\beta = 1.90$ on a $32^3 \times 64$ lattice.

Our aim is to replicate the physical aspects of the PACS-CS configurations [43] used in the analysis of the nucleon spectrum in full QCD [2]. We aim to explore the nucleon spectrum in a quenched simulation with matched lattice spacing and quark masses to evaluate the sensitivity of the $1s$ and $2s$ state energies observed on the lattice.

Thus, we seek the same $32^3 \times 64$ lattice volume. We consider the same $\mathcal{O}(a^2)$ -improved Iwasaki gauge-field action [45] with β tuned to provide a lattice spacing of $a = 0.100$ fm as determined via the Sommer scheme [38].

To access the same light quark masses in the quenched version of the theory, we use the fat-link clover action with three sweeps of stout-link smearing applied to the links [46] with an isotropic smearing parameter $\rho = 0.1$. With this, the mean link, $u_0 = \langle \text{tr} \square / 3 \rangle^{1/4} = 0.993$, such that mean-field improvement of the tree-level clover coefficient, $C_{\text{SW}} = 1$ is sufficient to obtain $\mathcal{O}(a)$ improvement of this Wilson-type action. The use of fat links in the action addresses the exceptional configuration problem associated with large additive mass renormalisations which otherwise make the simulations at the lightest quark mass untenable in the quenched theory. The hopping parameters of this fermion action in the pure gauge theory are tuned to replicate the pion masses realised in the PACS-CS simulations [43]. These tuned parameters are summarised in Table 1.

To enhance statistics, we consider multiple fermion sources on each of the 2+1 flavour gauge field configurations, as summarised in Table 1. Configurations are circularly shifted in space and time directions after which a fixed boundary condition is introduced at $t = N_t = 64$. We place the fermion source away from the boundary at $t_s = N_t/4 = 16$ such that masses extracted at large Euclidean time are maximally displaced from the boundary.

Our selection of a fixed boundary condition prevents states from wrapping around the lattice. This enables a careful examination of the exponential time dependence without significant artefacts. Only the pion correlator lives long enough to reveal the effect of the fixed boundary condition in our simulations and this occurs after $t = N_t 3/4 = 48$ where the pion effective mass systematically rises just more than one standard deviation above the normal fluctuations observed. The ground-state nucleon correlator does not survive long enough to see this boundary effect. No systematic drift is observed in the correlator prior to signal loss.

To enhance the basis of interpolating fields employed in our variational analysis, gauge-invariant

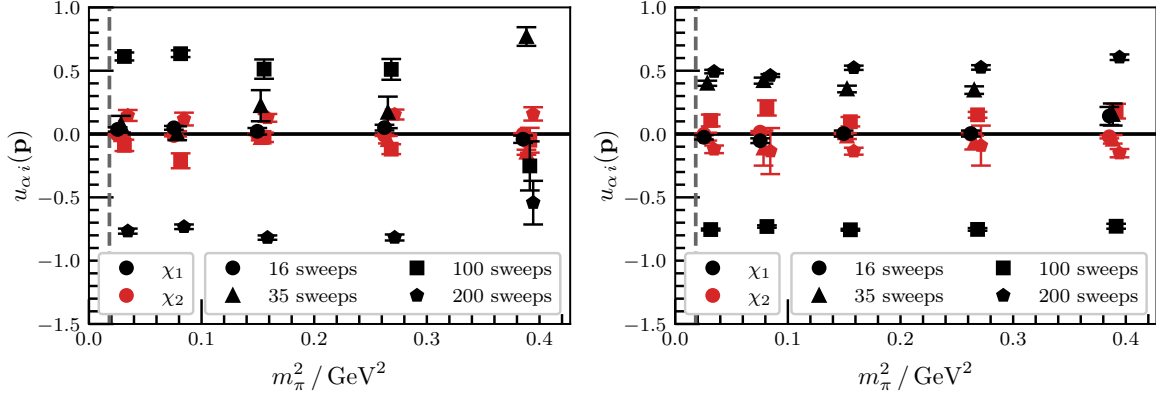


Figure 1. Eigenvector components $u_{\alpha i}(\mathbf{p})$ for the $2s$ (left) and $3s$ (right) nucleon excitations in full 2+1 flavour QCD at momentum $\mathbf{p} = \mathbf{0}$ at the five quark masses of the PACS-CS ensembles [43]. Here the index i runs over eight values for the two interpolators, χ_1 and χ_2 , times the four different gauge invariant Gaussian smearing [39] levels, 16, 35, 100 and 200 sweeps as discussed in the text.

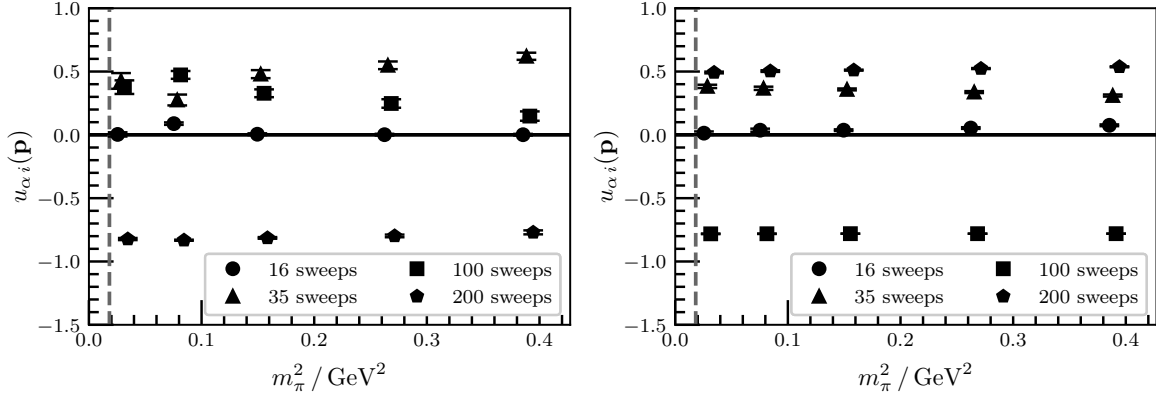


Figure 2. Eigenvector components $u_{\alpha i}(\mathbf{p})$ for the $2s$ (left) and $3s$ (right) positive parity nucleon excitations in quenched QCD at momentum $\mathbf{p} = \mathbf{0}$. Calculations are performed at κ_Q values tuned to reproduce the five quark masses of the PACS-CS ensembles [43]. Here the index i runs over the four different gauge invariant Gaussian smearing [39] levels, 16, 35, 100 and 200 sweeps for the interpolator, χ_1 .

Gaussian smearing [39] is used at the fermion source and sink with a fixed smearing fraction and four different smearing levels. Following the results of the early comprehensive analyses of Refs. [47, 47], we consider 16, 35, 100, and 200 smearing sweeps with a smearing fraction of $\alpha = 0.7$. Variational parameters are fixed at $t_0 = t_s + 1$ and $\Delta t = 2$, except for the second lightest mass, where $\Delta t = 3$ is used to avoid a degeneracy in the variational analysis.

4. Excitation properties

4.1. Interpolating fields

We begin with an examination of the role of the correlation matrix interpolating fields in exciting the $2s$ state observed in our full QCD simulations. Figure 1 illustrates the eigenvector components $u_{\alpha i}(\mathbf{p})$ for the $2s$ (left) and $3s$ (right) nucleon excitations, at momentum $\mathbf{p} = \mathbf{0}$ at the five quark masses of the PACS-CS ensembles. Here the index i runs over eight values for the two interpolators, χ_1 and χ_2 , times the four different gauge invariant Gaussian smearing levels, 16, 35, 100 and 200 sweeps.

The first feature to note is that the interpolator χ_2 plays a negligible role in exciting either radial excitation. It was dropped in the wave function analyses of Refs. [7, 8] with little effect. The insensitivity of the spectrum obtained with our single-state ansatz is well documented [9, 10, 47, 47]. While the presence or absence of a state does indeed depend on the interpolating fields used to form the correlation matrix, the energy of the observed excitation is not sensitive.

In the quenched theory, flavour-singlet dressings of hadron states can become problematic at the lighter quark masses considered. Upon quenching the theory, the η' meson remains degenerate with the pion, and its two-loop disconnected quark-flow structure generates negative metric contributions that can render correlation functions that would be positive definite in the full theory negative. By dropping χ_2 from the quenched analysis, we are able to minimise coupling to these problematic contributions.

The second main feature to be drawn from Fig. 1, is that the $2s$ state's node structure is predominantly governed through the interplay between the 100 and 200 sweep interpolators. The familiar superposition of broad and narrow distributions with a relative minus sign [6, 48, 49] forms a single node in the wave function [7, 8], a signature of this state. It's interesting that at the heaviest quark mass considered, the central peak is narrower, this time superposing a narrow 35 sweep source with a linear combination of broader 100 and 200 sweep sources with signs opposite the central 35 sweep source.

Turning now to the $3s$ excitation, we observe sign changes from the narrow 35 sweep source, to the 100 sweep source and again from the 100 sweep source to the 200 sweep source, thus creating two nodes in the wave function. Once again a narrowing is observed in the central peak at the heaviest quark mass, with the 16 sweep source combining with the 35 sweep source.

Proceeding to the quenched theory, we observe the same general structure where narrow sources are superposed with broad sources to create nodes in the wave function. Figure 2 illustrates the eigenvectors for the $2s$ (left) and $3s$ (right) excitations.

We begin with consideration of the $2s$ excitation. This time the broad 200 sweep source is superposed with a linear combination of narrower sources with signs opposite to the broad source. Again, a single node is produced. It is interesting to see the more enhanced role for the narrower 35 sweep source at the second-heaviest quark mass. This state is smaller in the quenched theory, in accord with a suppression of meson-baryon couplings. Moreover, the quark mass dependence of the size of the inner peak, driven by interplay between 35 and 100 sweeps is in accord with expectations. At the heaviest quark mass, 35 sweeps plays the dominate role as in full QCD, but the 100 sweep interpolator comes into play more as the quarks become light. Thus, at the lighter quark masses considered, the change in the structure of the quenched states is more subtle.

The $3s$ excitation displays a very similar set of eigenvectors to the full QCD simulations. The only notable difference is that there is less narrowing at the heaviest quark mass. We note that for both states considered here, the 16 sweep source plays only a small role. In every case its sign matches the 35 sweep source such that there is no chance of it creating an additional node in the wave function.

4.2. Nucleon mass spectrum

With this understanding of how the correlation matrix is acting to excite the states of interest, we now turn to a careful examination of the nucleon spectrum. Figure 3 shows the ground-state nucleon mass and the first two radial excitations as a function of quark mass for both full $2+1$ flavour QCD (black points) and for the quenched theory (blue points).

The mass of the ground state nucleon is observed to be insensitive to the change in the meson dressing of the nucleon at all but the lightest quark mass considered. Here, the single-particle dominated state is pushed down in the process of mixing with the more energetic two-particle πN states in full QCD. The suppression of these couplings in the quenched theory suppresses this mixing, leaving the ground state relatively high.

While the energy of most excited states change more than 1σ , there are three states with relatively small uncertainties that remain invariant at the 1σ level upon quenching. The three states are at ~ 2 GeV at the lightest three quark masses. These are the $2s$ excitations of the nucleon that we have

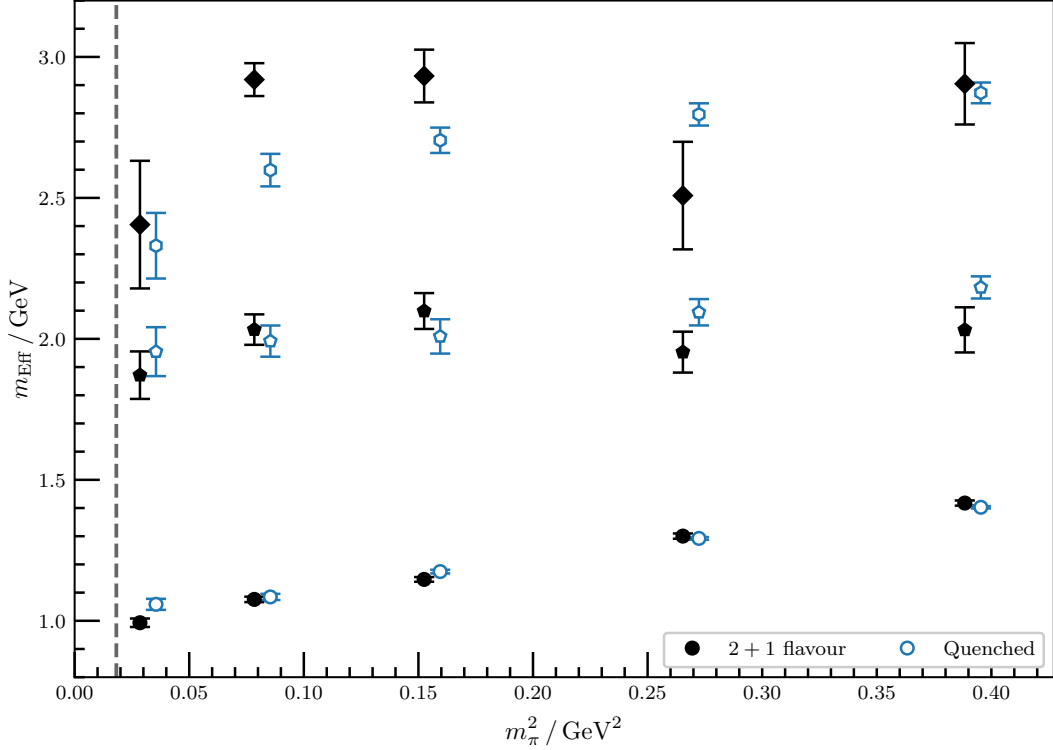


Figure 3. 1s, 2s and 3s nucleon mass spectrum observed in lattice QCD calculations in full 2+1 flavour QCD (filled symbols) and quenched QCD (open symbols). While the energy of most excitations change more than 1σ , the three states at ~ 2 GeV for the lightest three quark masses remain invariant at the 1σ level upon quenching.

hypothesised should be insensitive if the 2s excitation is indeed associated with the $N1/2^+(1710)$ and $N1/2^+(1880)$ resonances. The small width of the $N1/2^+(1710)$ suggests invariance due to the small coupling to meson-baryon channels. Similarly, the need for photoproduction to see the $N1/2^+(1880)$ resonance again suggests a diminished sensitivity to changes in the meson-baryon dressings of the 2s state. This has now been realised, but only at light quark masses approaching the physical point.

At the two largest quark masses considered, the variation of the spectrum is larger. Here HEFT can provide some insight into why the variance is more significant. HEFT describes the lowest-lying excitations at the two largest quark masses as having strong mixings with the πN two-particle basis states [22] as they pass through the lattice QCD points. At the largest quark mass, the first πN two particle basis state is higher in energy than the state observed on the lattice. The mixing of the single and two-particle states acts to push down the single particle dominated state in full QCD. The process of quenching suppresses the couplings between N and πN and weaker mixing with the higher πN basis states causes the quenched results to sit higher.

5. Conclusion

In summary, we have presented evidence that there are indeed quark-model like states in the nucleon spectrum. While the positions of the $N1/2^+(1710)$ and $N1/2^+(1880)$ resonances in the nucleon spectrum are close to the 2s excitation observed in lattice QCD, making them plausible candidates, we now have additional information suggesting these resonances are associated with the 2s excitation.

We have argued the physical properties of these resonances provide additional insight. The small width of the $N1/2^+(1710)$ suggests a relatively small coupling to meson-baryon channels such that

the position of the $2s$ state in the spectrum should be largely invariant to changes in the strength of meson-baryon dressings of the state. This is echoed by the need for photoproduction to see the $N1/2^+(1880)$ resonance. Again this property suggests a diminished coupling to meson-baryon states and thus invariance of the $2s$ state energy upon suppressing the strength of meson-baryon dressings of the state.

To alter the couplings of two-particle meson-baryon states forming the meson cloud of lattice energy eigenstates, we have resorted to quenching the theory, removing sea-quark-loop contributions and thus altering and generally suppressing the meson cloud contributions to eigenstates observed in quenched lattice calculations. The anticipated approximate invariance of the $2s$ state seen in lattice QCD simulations has now been observed at light quark masses approaching the physical point.

The eigenvectors of the lattice variational method describe these radial excitations of quenched and full QCD in a consistent manner. The first and second excitations have one and two nodes respectively. Moreover, the quark mass dependence of the node radius is in accord with expectations with heavier quark masses corresponding to smaller radii. While the quenched states do tend to be smaller in some cases, the change is subtle at the lightest quark masses as the 100 sweep smearing interpolator comes into play.

In interpreting and understanding the lattice results, we have drawn on results from Hamiltonian Effective Field Theory which provides insight into the composition of baryon excitations in terms of the superposition of basis states required to construct the eigenstates of the Hamiltonian. Of particular interest is the prediction of states near 2 GeV dominated by single-particle contributions [22] to the extent that their properties are expected to be insensitive to changes in the meson-baryon couplings. This expectation has been observed in our lattice QCD simulations. At larger quark masses where the first excitation observed in lattice QCD has a larger πN component [22], significant movement in the mass of the state is anticipated and observed.

We note that the masses of these radial excitations in the quenched theory remain far from the Roper resonance energy further supporting the contemporary perspective that the structure of the Roper is complicated and beyond the scope of a conventional quark model radial excitation.

Consequentially, accessing finite-volume states in the region of the Roper resonance requires the consideration of non-local momentum-projected two-particle interpolating fields, similar to what has been done for the $\Lambda(1405)$ [50, 51]. As such, the determination of the electromagnetic form factors and transition moments of the Roper demand three-point function techniques on momentum projected five-quark correlation functions, presenting a significant challenge to the community.

Associating the $2s$ excitation with the $N1/2^+(1710)$ and $N1/2^+(1880)$ resonances also provides a resolution to the missing baryon resonances problem [14, 52]. Had the parameters of the quark model been tuned to place the $2s$ excitation at ~ 2 GeV, the next excitation would be well above 2 GeV. In this regard, the missing resonance problem may be regarded as further evidence that the $2s$ radial excitation of the nucleon is not associated with the Roper resonance, but rather the $N1/2^+(1710)$ and $N1/2^+(1880)$ resonances.

Acknowledgments

We thank the PACS-CS Collaboration for making their configurations available via the International Lattice Data Grid (ILDG). This research was supported with supercomputing resources provided by the Phoenix HPC service at the University of Adelaide. This research was undertaken with the assistance of resources from the National Computational Infrastructure (NCI), provided through the National Computational Merit Allocation Scheme, and supported by the Australian Government through Grant No. LE190100021 via the University of Adelaide Partner Share. This research was supported by the Australian Research Council through Grants No. DP150103164, DP190102215 and DP210103706 (DBL). WK was supported by the Pawsey Supercomputing Centre through the Pawsey Centre for Extreme Scale Readiness (PaCER) program. FS is supported by a Ramsay Fellowship from the University of Adelaide.

References

- [1] Derek Leinweber, Waseem Kamleh, Adrian Kiratidis, Zhan-Wei Liu, Selim Mahbub, Dale Roberts, Finn Stokes, Anthony W. Thomas, and Jiajun Wu. N^* Spectroscopy from Lattice QCD: The Roper Explained. *JPS Conf. Proc.*, 10:010011, 2016. [arXiv:1511.09146](#), [doi:10.7566/JPSCP.10.010011](#).
- [2] Zhan-Wei Liu, Waseem Kamleh, Derek B. Leinweber, Finn M. Stokes, Anthony W. Thomas, and Jia-Jun Wu. Hamiltonian effective field theory study of the $N^*(1440)$ resonance in lattice QCD. *Phys. Rev. D*, 95(3):034034, 2017. [arXiv:1607.04536](#), [doi:10.1103/PhysRevD.95.034034](#).
- [3] M. Selim Mahbub, Waseem Kamleh, Derek B. Leinweber, Peter J. Moran, and Anthony G. Williams. Roper Resonance in 2+1 Flavor QCD. 2010. (Published in [4]). [arXiv:1011.5724v1](#).
- [4] M. Selim Mahbub, Waseem Kamleh, Derek B. Leinweber, Peter J. Moran, and Anthony G. Williams. Roper Resonance in 2+1 Flavor QCD. *Phys. Lett. B*, 707:389–393, 2012. [arXiv:1011.5724](#), [doi:10.1016/j.physletb.2011.12.048](#).
- [5] C. Alexandrou, T. Leontiou, C. N. Papanicolas, and E. Stiliaris. Novel analysis method for excited states in lattice QCD: The nucleon case. *Phys. Rev. D*, 91(1):014506, 2015. [arXiv:1411.6765](#), [doi:10.1103/PhysRevD.91.014506](#).
- [6] M. Selim Mahbub, Waseem Kamleh, Derek B. Leinweber, Peter J. Moran, and Anthony G. Williams. Structure and Flow of the Nucleon Eigenstates in Lattice QCD. *Phys. Rev. D*, 87(9):094506, 2013. [arXiv:1302.2987](#), [doi:10.1103/PhysRevD.87.094506](#).
- [7] Dale S. Roberts, Waseem Kamleh, and Derek B. Leinweber. Wave Function of the Roper from Lattice QCD. *Phys. Lett. B*, 725:164–169, 2013. [arXiv:1304.0325](#), [doi:10.1016/j.physletb.2013.06.056](#).
- [8] Dale S. Roberts, Waseem Kamleh, and Derek B. Leinweber. Nucleon Excited State Wave Functions from Lattice QCD. *Phys. Rev. D*, 89(7):074501, 2014. [arXiv:1311.6626](#), [doi:10.1103/PhysRevD.89.074501](#).
- [9] Adrian L. Kiratidis, Waseem Kamleh, Derek B. Leinweber, and Benjamin J. Owen. Lattice baryon spectroscopy with multi-particle interpolators. *Phys. Rev. D*, 91:094509, 2015. [arXiv:1501.07667](#), [doi:10.1103/PhysRevD.91.094509](#).
- [10] Adrian L. Kiratidis, Waseem Kamleh, Derek B. Leinweber, Zhan-Wei Liu, Finn M. Stokes, and Anthony W. Thomas. Search for low-lying lattice QCD eigenstates in the Roper regime. *Phys. Rev. D*, 95(7):074507, 2017. [arXiv:1608.03051](#), [doi:10.1103/PhysRevD.95.074507](#).
- [11] Tanjib Khan, David Richards, and Frank Winter. Positive-parity baryon spectrum and the role of hybrid baryons. *Phys. Rev. D*, 104(3):034503, 2021. [arXiv:2010.03052](#), [doi:10.1103/PhysRevD.104.034503](#).
- [12] C. B. Lang, L. Leskovec, M. Padmanath, and S. Prelovsek. Pion-nucleon scattering in the Roper channel from lattice QCD. *Phys. Rev. D*, 95(1):014510, 2017. [arXiv:1610.01422](#), [doi:10.1103/PhysRevD.95.014510](#).
- [13] Finn M. Stokes, Waseem Kamleh, and Derek B. Leinweber. Elastic Form Factors of Nucleon Excitations in Lattice QCD. *Phys. Rev. D*, 102(1):014507, 2020. [arXiv:1907.00177](#), [doi:10.1103/PhysRevD.102.014507](#).
- [14] Liam Hockley, Waseem Kamleh, Derek Leinweber, and Anthony Thomas. Searching for the first radial excitation of the $\Delta(1232)$ in lattice QCD. *J. Phys. G*, 51(6):065106, 2024. [arXiv:2312.11574](#), [doi:10.1088/1361-6471/ad33e2](#).
- [15] L. David Roper. Evidence for a P-11 Pion-Nucleon Resonance at 556 MeV. *Phys. Rev. Lett.*, 12:340–342, 1964. [doi:10.1103/PhysRevLett.12.340](#).
- [16] Christopher Michael. Adjoint Sources in Lattice Gauge Theory. *Nucl. Phys. B*, 259:58–76, 1985. [doi:10.1016/0550-3213\(85\)90297-4](#).
- [17] Martin Lüscher and Ulli Wolff. How to Calculate the Elastic Scattering Matrix in Two-dimensional Quantum Field Theories by Numerical Simulation. *Nucl. Phys. B*, 339:222–252, 1990. [doi:10.1016/0550-3213\(90\)90540-T](#).
- [18] Robert G. Edwards et al. Excited state baryon spectroscopy from lattice QCD. *Phys. Rev. D*, 84:074508, 2011. [arXiv:1104.5152](#), [doi:10.1103/PhysRevD.84.074508](#).
- [19] Benjamin J. Menadue, Waseem Kamleh, Derek B. Leinweber, M. Selim Mahbub, and Benjamin J. Owen. Electromagnetic Form Factors for the $\Lambda(1405)$. *PoS, LATTICE2013:280*, 2014. [arXiv:1311.5026](#), [doi:10.22323/1.187.0280](#).
- [20] Jonathan M. M. Hall, Waseem Kamleh, Derek B. Leinweber, Benjamin J. Menadue, Benjamin J. Owen, Anthony W. Thomas, and Ross D. Young. Lattice QCD Evidence that the $\Lambda(1405)$ Resonance is an Antikaon-Nucleon Molecule. *Phys. Rev. Lett.*, 114(13):132002, 2015. [arXiv:1411.3402](#), [doi:10.1103/PhysRevLett.114.132002](#).
- [21] Jonathan M. M. Hall, Waseem Kamleh, Derek B. Leinweber, Benjamin J. Menadue, Benjamin J. Owen, and Anthony W. Thomas. Light-quark contributions to the magnetic form factor of the $\Lambda(1405)$. *Phys. Rev. D*, 95(5):054510, 2017. [arXiv:1612.07477](#), [doi:10.1103/PhysRevD.95.054510](#).
- [22] Jia-jun Wu, Derek B. Leinweber, Zhan-wei Liu, and Anthony W. Thomas. Structure of the Roper Resonance from Lattice QCD Constraints. *Phys. Rev. D*, 97(9):094509, 2018. [arXiv:1703.10715](#), [doi:10.1103/PhysRevD.97.094509](#).
- [23] John Bulava et al. Low-lying baryon resonances from lattice QCD. *Nuovo Cim. C*, 47(4):165, 2024. [arXiv:2310.08375](#), [doi:10.1393/ncc/i2024-24165-1](#).
- [24] Colin Morningstar, John Bulava, Andrew D. Hanlon, Ben Hörz, Daniel Mohler, Amy Nicholson, Sarah Skinner, and André Walker-Loud. Progress on Meson-Baryon Scattering. *PoS, LATTICE*, 2021:170, 2022. [arXiv:2111.07755](#), [doi:10.22323/1.396.0170](#).
- [25] John Bulava, Andrew D. Hanlon, Ben Hörz, Colin Morningstar, Amy Nicholson, Fernando Romero-López, Sarah Skinner, Pavlos Vranas, and André Walker-Loud. Elastic nucleon-pion scattering at $m_\pi = 200$ MeV from lattice

- QCD. *Nucl. Phys. B*, 987:116105, 2023. [arXiv:2208.03867](#), [doi:10.1016/j.nuclphysb.2023.116105](#).
- [26] Adam Virgili, Waseem Kamleh, and Derek Leinweber. Role of chiral symmetry in the nucleon excitation spectrum. *Phys. Rev. D*, 101(7):074504, 2020. [arXiv:1910.13782](#), [doi:10.1103/PhysRevD.101.074504](#).
- [27] Finn M. Stokes, Waseem Kamleh, Derek B. Leinweber, M. Selim Mahbub, Benjamin J. Menadue, and Benjamin J. Owen. Parity-expanded variational analysis for nonzero momentum. *Phys. Rev. D*, 92(11):114506, 2015. [arXiv:1302.4152](#), [doi:10.1103/PhysRevD.92.114506](#).
- [28] Finn M. Stokes, Waseem Kamleh, and Derek B. Leinweber. Structure and transitions of nucleon excitations via parity-expanded variational analysis. *PoS, LATTICE*, 2019:182, 2019. [arXiv:2001.07919](#), [doi:10.22323/1.363.0182](#).
- [29] A. V. Anisovich et al. Strong evidence for nucleon resonances near 1900 MeV. *Phys. Rev. Lett.*, 119(6):062004, 2017. [arXiv:1712.07549](#), [doi:10.1103/PhysRevLett.119.062004](#).
- [30] S. Navas et al. Review of particle physics. *Phys. Rev. D*, 110(3):030001, 2024. [doi:10.1103/PhysRevD.110.030001](#).
- [31] James N. Labrenz and Stephen R. Sharpe. Quenched chiral perturbation theory for baryons. *Phys. Rev. D*, 54:4595–4608, 1996. [arXiv:hep-lat/9605034](#), [doi:10.1103/PhysRevD.54.4595](#).
- [32] J. M. M. Hall and D. B. Leinweber. Flavor-singlet baryons in the graded symmetry approach to partially quenched QCD. *Phys. Rev. D*, 94(9):094004, 2016. [arXiv:1509.08226](#), [doi:10.1103/PhysRevD.94.094004](#).
- [33] Derek B. Leinweber. Quark contributions to baryon magnetic moments in full, quenched and partially quenched QCD. *Phys. Rev. D*, 69:014005, 2004. [arXiv:hep-lat/0211017](#), [doi:10.1103/PhysRevD.69.014005](#).
- [34] Derek B. Leinweber and Anthony W. Thomas. Sea-quark loop contributions to the d^-u^- asymmetry in the proton. *Phys. Rev. D*, 109(3):L031503, 2024. [arXiv:2211.13423](#), [doi:10.1103/PhysRevD.109.L031503](#).
- [35] S. Aoki et al. Quenched light hadron spectrum. *Phys. Rev. Lett.*, 84:238–241, 2000. [arXiv:hep-lat/9904012](#), [doi:10.1103/PhysRevLett.84.238](#).
- [36] S. Aoki et al. Light hadron spectrum and quark masses from quenched lattice QCD. *Phys. Rev. D*, 67:034503, 2003. [arXiv:hep-lat/0206009](#), [doi:10.1103/PhysRevD.67.034503](#).
- [37] Zoltan Fodor and Christian Hoelbling. Light Hadron Masses from Lattice QCD. *Rev. Mod. Phys.*, 84:449, 2012. [arXiv:1203.4789](#), [doi:10.1103/RevModPhys.84.449](#).
- [38] R. Sommer. A New way to set the energy scale in lattice gauge theories and its applications to the static force and α_s in SU(2) Yang-Mills theory. *Nucl. Phys. B*, 411:839–854, 1994. [arXiv:hep-lat/9310022](#), [doi:10.1016/0550-3213\(94\)90473-1](#).
- [39] S. Gusken. A Study of smearing techniques for hadron correlation functions. *Nucl. Phys. B Proc. Suppl.*, 17:361–364, 1990. [doi:10.1016/0920-5632\(90\)90273-W](#).
- [40] Bradley Efron. Computers and the Theory of Statistics: Thinking the Unthinkable. *SIAM Review*, 21(4):460–480, 1979. [doi:10.1137/1021092](#).
- [41] M. Selim Mahbub, Waseem Kamleh, Derek B. Leinweber, Peter J. Moran, and Anthony G. Williams. Low-lying Odd-parity States of the Nucleon in Lattice QCD. *Phys. Rev. D*, 87(1):011501, 2013. [arXiv:1209.0240](#), [doi:10.1103/PhysRevD.87.011501](#).
- [42] M. Selim Mahbub, Waseem Kamleh, Derek B. Leinweber, and Anthony G. Williams. Searching for low-lying multi-particle thresholds in lattice spectroscopy. *Annals Phys.*, 342:270–282, 2014. [arXiv:1310.6803](#), [doi:10.1016/j.aop.2014.01.004](#).
- [43] S. Aoki et al. 2+1 Flavor Lattice QCD toward the Physical Point. *Phys. Rev. D*, 79:034503, 2009. [arXiv:0807.1661](#), [doi:10.1103/PhysRevD.79.034503](#).
- [44] Mark G. Beckett, Balint Joo, Chris M. Maynard, Dirk Pleiter, Osamu Tatebe, and Tomoteru Yoshie. Building the International Lattice Data Grid. *Comput. Phys. Commun.*, 182:1208–1214, 2011. [arXiv:0910.1692](#), [doi:10.1016/j.cpc.2011.01.027](#).
- [45] Y. Iwasaki. Renormalization group analysis of lattice theories and improved lattice action: Two-dimensional nonlinear O(N) sigma model. *Nucl. Phys. B*, 258:141–156, 1985. [doi:10.1016/0550-3213\(85\)90606-6](#).
- [46] Peter J. Moran, Derek B. Leinweber, and Jianbo Zhang. Wilson mass dependence of the overlap topological charge density. *Phys. Lett. B*, 695:337–342, 2011. [arXiv:1007.0854](#), [doi:10.1016/j.physletb.2010.11.005](#).
- [47] M. S. Mahbub, Alan O Cais, Waseem Kamleh, Ben G. Lasscock, Derek B. Leinweber, and Anthony G. Williams. Isolating the Roper Resonance in Lattice QCD. *Phys. Lett. B*, 679:418–422, 2009. [arXiv:0906.5433](#), [doi:10.1016/j.physletb.2009.07.063](#).
- [48] Liam Hockley, Waseem Kamleh, Derek Leinweber, and Anthony Thomas. Δ Baryon Spectroscopy in Lattice QCD. *Few Body Syst.*, 64(3):46, 2023. [arXiv:2304.10187](#), [doi:10.1007/s00601-023-01832-x](#).
- [49] Liam Hockley, Waseem Kamleh, Derek Leinweber, and Anthony Thomas. Exploring the Ω^- spectrum in lattice QCD. *J. Phys. G*, 8 2024. [arXiv:2408.16281](#).
- [50] John Bulava et al. Two-Pole Nature of the $\Lambda(1405)$ resonance from Lattice QCD. *Phys. Rev. Lett.*, 132(5):051901, 2024. [arXiv:2307.10413](#), [doi:10.1103/PhysRevLett.132.051901](#).
- [51] John Bulava et al. Lattice QCD study of $\pi\Sigma$ - K^-N scattering and the $\Lambda(1405)$ resonance. *Phys. Rev. D*, 109(1):014511, 2024. [arXiv:2307.13471](#), [doi:10.1103/PhysRevD.109.014511](#).
- [52] Derek B. Leinweber, Curtis D. Abell, Liam C. Hockley, Waseem Kamleh, Zhan-Wei Liu, Finn M. Stokes, Anthony W. Thomas, and Jia-Jun Wu. Understanding the nature of baryon resonances. *Nuovo Cim. C*, 47(4):146, 2024. [arXiv:2401.04901](#), [doi:10.1393/ncc/i2024-24146-4](#).